USE OF INELASTIC STRAIN AS A BASIS FOR ANALYZING THERMOMECHANICAL TEST DATA

P.A. Bartolotta and J.R. Ellis
NASA Lewis Research Center
Cleveland, Ohio

Experimental investigations of isothermal and thermomechanical material behavior have been conducted for many years (refs. 1 to 5). In these investigations, comparisons of general material behavior trends have been made utilizing data collected by strip chart recordings and x-y plots. Typically, these comparisons were usually drawn from data in the form of stress range versus cycles. This method was useful to identify general material hardening characteristics, but totally ignored the wealth of information about inelastic material response throughout a cycle. Inelastic material response can be used to give insight to isothermal and thermomechanical behavior in a form that is more consistent with constitutive equation development. Likewise, other traditional approaches for data representation (i.e., tensile or compressive stress amplitude versus cycle, number of cycles to failure versus inelastic strain range, etc.) are useful and necessary to identify general material trends, but fail to illustrate the material's inelastic response. To obtain any other information such as inelastic strain-time response or inelastic strain rate – stress plots were time consuming and cumbersome. The task of obtaining this information usually entailed either hand calculations or, if a computer was going to be used, the data from the strip charts (or x-y plots) needed to be digitized. One possible solution to this problem is to use a computer system to acquire and manipulate experimental data. Therefore, recent efforts at NASA Lewis Research Center under the HOST program have been focused on the development of improved acquisition and representation of experimental data. In this paper a new approach for data representation will be introduced. A brief discussion about new thermomechanical testing systems recently installed at Lewis will also be presented. Finally, preliminary comparisons of thermomechanical and isothermal data using inelastic strain response will be presented.

EXPERIMENTAL DETAIL

The equipment and procedures used in the isothermal experiments have been previously described in detail (ref. 4). These experiments were conducted under uniaxial loading on closed-loop, electrohydraulic test systems. The specimens tested had a 3.175-cm parallel working section with a 0.795-cm outside diameter. Strains were measured over a 2.54-cm gage length using an axial extensometer. The specimens were heated using an RF induction heater and considerable effort was extended in achieving uniform temperature profiles over the gage length. Usually, temperatures fell within ±5 °C of the nominal test temperature throughout the experiments.

The isothermal experiments were performed in strain control over a longitudinal strain range ($\Delta\varepsilon_t$) of ±0.3 percent at a constant strain rate ($\dot{\varepsilon}_t$) of 10^{-4} sec^{-1}. Stress and strain responses as a function of time were recorded using both a strip chart recorder and a Bascom-Turner recorder. The Bascom-Turner system was programmed to acquire data at predetermined intervals.

Thermomechanical tests were conducted utilizing new digitally controlled electro-hydraulic test systems. These test systems are described in detail in reference 6. Special features of these systems include

(1) Hydraulic actuator bearings for maintaining alignment throughout the length of the stroke

(2) Hydraulic water-cooled grips for assured specimen alignment and ease of specimen installation

(3) Dual servo-valves for high system fidelity

Specimens were again heated using an RF induction heater. Specimen cooling was by means of the test system's water-cooled grips. This was the preferred approach as it allowed temperature profiles to be maintained within acceptable limits during the cooling process. Also to assist in this regard, the gage length over which strain measurements were made was reduced to 1.27 cm in these experiments. The net result was that temperatures in the specimen's gage length were within ±10 °C of programmed values during temperature cycling.

A Data General S/20 microcomputer was used for control purposes and data acquisition. Total strains ε_t and strain rate $\dot{\varepsilon}_t$ were programmed such that the mechanical strain range $\Delta\varepsilon_m$ was maintained at ±0.3 percent with a constant mechanical strain rate $\dot{\varepsilon}_m$ of 10^{-4} sec^{-1}. Both mechanical strains and temperature were programmed to follow triangular waveforms which were 180° out-of-phase. Temperature rates were held constant at 200 °C min^{-1}. Due to time limitations, tests were conducted for 5000 cycles unlike the isothermal tests which were conducted until fatigue failure occurred.

The following test procedures were adopted for the thermomechanical experiments:

(1) Static thermal profiles were achieved for the median temperature.

(2) In load control with zero load, the temperature was then cycled and the thermal strain-temperature response was recorded.

(3) For the maximum, mean, and minimum temperatures, the elastic modulus was found by carefully cycling the load such that the material response remained elastic.

(4) Finally, the thermomechanical test was started. Mechanical strain range and rates were controlled using information obtained in step (2).

(5) After 5000 cycles the test was stopped and the specimen was brought back to a zero-stress, zero-strain state.

(6) Procedures (2) and (3) were again conducted.

The material under investigation was Hastelloy-X in the solution annealed condition. Hastelloy-X is an austenitic nickel-based superalloy used in gas turbine components that require oxidation resistance up to 1200 °C. The material was obtained in 0.19 mm o.d. bar form, meeting the requirements of Aerospace Material Specification (AMS) 5754H. Overall specimen geometry for the thermomechanical experiments was the same as the specimens used for the isothermal tests except that

the gripping ends were smooth shanks instead of threaded. Smooth shank ends exhibit better alignment characteristics along with efficient heat transfer characteristics. Surface finish for these specimens was 16 rms.

DATA MANIPULATION

The key components of the data manipulation scheme adopted for both isothermal and thermomechanical data are the computer test system and its network. Figure 1 illustrates schematically the computer test system used for this study. This system consists of a 32-bit superminicomputer which serves as the host for 14 other 16-bit satellite minicomputers. The satellite minicomputer is presently used as an expert waveform generator to control both mechanical loading and specimen temperature. The satellites are also used for data acquisition. Data including strain, stress, and specimen temperature are collected at a constant sampling rate that is set for 500 observations per predetermined cycle, and are stored on the satellite's hard disk. Once the test is over, the test data is transferred over to the host computer where it is stored on both hard disk and magnetic tape. The data can be manipulated either by the host computer or by a personal computer (PC). For this study, the PC was chosen for the following reasons:

(1) The PC is equipped with graphics terminal and plotters for ease of data analysis.
(2) The PC has a "user friendly" statistical graphics software package.

The experimental data are transferred to the PC via a laboratory network line. This same link can be utilized in such a way that the PC can become a terminal for either the host or one of the satellite computers, thus making it easy to check on an experiment's progress from the researcher's desk.

The approach adopted for analyzing the isothermal data was as follows:

(1) Stress-strain hysteresis loops were partitioned into upper and lower halves at the reversal peaks.

      (a) Upper half - started at the compressive peak and ended at the tensile peak
      (b) Lower half - started at the tensile peak and ended at the compressive peak

(2) Time references were created at the reversal peaks.

      (a) Upper half - time origin located at compressive peak
      (b) Lower half - time origin located at tensile peak

(3) Inelastic strains were calculated for each half by

$$\varepsilon_{in} = \varepsilon_t - \sigma/E$$

where ε_{in} is the inelastic strain, ε_t is the total strain, σ is the associated stress, and E is the elastic modulus calculated from the first quarter cycle of the test.

(4) Inelastic strain-time response was plotted (fig. 2) for each half of the cycle.

(5) From these plots inelastic strain maxima (or minima) were located along with their corresponding time ($t = \text{time}_{\text{max/min}}$).

(6) From $0 \leq t \leq \text{time}_{\text{max/min}}$ a second order polynomial fit was used on the inelastic strain-time curve. And from $\text{time}_{\text{max/min}} \leq t \leq \text{time}_{\text{end}}$ a third order polynomial was used.

(Note: Two constraints were imposed for both fits. First at $t = \text{time}_{\text{max/min}}$, $\varepsilon_{\text{in}} = \varepsilon_{\text{in,max/min}}$ and secondly at $t = \text{time}_{\text{max/min}}$, $\varepsilon_{\text{in}} = 0$.)

(7) Fitting constants for both halves of the cycle were tabulated in the form shown in tables I and II.

To analyze the thermomechanical data, the approach adopted was similar to that adopted for the isothermal data except that the apparent strains (thermal strains) had to be accounted for and the elastic modulus is now a function of temperature. The procedures for this approach were as follows:

(1) An apparent strain-temperature function was formulated and used to find mechanical strains ε_m:

$$\varepsilon_m = \varepsilon_t - \varepsilon_a(T)$$

where $\varepsilon_a(T)$ is the apparent strain as a function of temperature.

(2) Two linear functions for the elastic modulus-temperature relationships were formulated. This was accomplished by calculating the elastic moduli for the upper, middle, and lower temperatures for each specimen by test procedures (3) and (6). The two lines were then fitted between the elastic modulus-temperature pairs.

(3) Inelastic strains were calculated by

$$\varepsilon_{\text{in}} = \varepsilon_m - \sigma/E(T)$$

Because of the unique shape of the inelastic strain-time response the same approach used for the isothermal fitting could not be adopted for the thermomechanical data fitting. Therefore, procedures need to be developed. Unfortunately, at this time the routine is still being formulated and is not ready for this publication.

RESULTS AND DISCUSSION

Results obtained from a 425 °C isothermal experiment and its fitted relationships are shown in figures 3 to 8. Figures 3 to 5 compare the fitted and experimental data in two forms. The stress – total strain form was chosen to compare how well the fit reproduced a typical experimental hysteresis loop, while the stress – inelastic strain form was chosen to build confidence in calculating inelastic strain rates using the fit equations. The fitted data curves were obtained utilizing equations and constants from tables I and II as follows:

(1) The time length of a half cycle was found by taking the strain range and dividing it by the strain rate of the experiment.

(2) The time length was divided into equal time intervals of 0.24 sec.

(3) Total strain-time response was found for each time interval.

306

In general: $\varepsilon_t = \dot{\varepsilon}_t(t) + \varepsilon'_t$
upper half: $\varepsilon_t = 100 \ \mu\varepsilon(t) - 3000 \ \mu\varepsilon$
lower half: $\varepsilon_t = -100 \ \mu\varepsilon(t) + 3000 \ \mu\varepsilon$

where ε'_t is the total strain value located at the starting reversal peak.

(4) Likewise for each time interval, inelastic strain-time response was calculated from the equations and appropriate constants from tables I and II.

(5) Stresses were finally calculated for each interval.

$$\sigma = E \ (\varepsilon_t - \varepsilon_{in}) \ x \ 10^{-6}$$

Maximum differences between the experimental and fitted data are 50 $\mu\varepsilon$ for inelastic strains and 15 MPa for stresses. These error values are relatively low. In fact the fit appears to improve with increasing number of cycles. The applicability of this approach has been demonstrated on other isothermal experiments. However, in a few experiments slight variations in the orders of the polynomial equations are necessary.

One can differentiate the general fit equations (table I and II) and calculate inelastic strain rates with a reasonable level of confidence in the results. Figures 6 to 8 present curves of the stress-inelastic strain rate response of the same 425 °C isothermal data of figures 3 to 5. Expressing data in this form provides insight regarding the variation of inelastic strain rate during cycling. It should be noted that the stresses used in these plots are experimental values and the inelastic strain rates are the only calculated values.

The material hardening behavior and its relationship with inelastic strain rates are illustrated in figures 6 to 8. In these figures, the stress – inelastic strain response seems to be asymmetric about a skewed axis. Another trend illustrated by these figures is the way the two curve halves move closer together, finally meeting, as the material hardens. Also note that as the curves move closer together, the skewed axis of asymmetry seems to rotate counter-clockwise until parts of the curves at cycle 5000 become the skewed axis. At the present time, physical and theoretical interpretations of the information are being investigated by constitutive modelers at NASA Lewis Research Center.

Results obtained from two isothermal (205 and 425 °C) and one out-of-phase thermomechanical (200 to 400 °C) experiments are presented in figures 9 to 11. The thermomechanical test was conducted in such a way that the mechanical strain range and mechanical strain rate were similar to what was used for the isothermal experiments. Because of the temperature response limitations of the experiment itself, it should be noted that at the tensile peaks of each thermomechanical cycle, the temperature overshot its lower bound by –5 °C (195 instead of 200 °C).

From figure 9 it can be observed that at the tenth cycle of the isothermal tests the stress – inelastic strain responses are similar. As for the thermomechanical test, the stress – inelastic strain response is slightly different compared to the isothermal data. This is probably due to the difference in mechanical strain range caused by the temperature overshoot. As can be seen from figures 9 and 10, the stress – inelastic strain response for the thermomechanical experiments seems to follow more closely that of the lower temperature isothermal test. As cycling continues, the thermomechanical material response seems to start following that of

the higher temperature isothermal experiment. This observation was also observed in another thermomechanical experiment (400 - 600 °C), which suggests that this trend is a general material hardening characteristic, but further investigation will have to be conducted before this can be confirmed.

CONCLUSIONS

It has been shown from this study that the proposed data analysis method, based on inelastic strain-time response, can be used effectively to represent cyclic response at elevated temperatures for Hastelloy-X. A high level of confidence in this method was built by making comparisons of the experimental and fitted data in two forms (figs. 3 to 5). Because of this level in confidence, the analysis was taken one step further and inelastic strain rates were calculated from the derivatives of the fit equations. With the data in this form, constitutive modelers should gain insight towards understanding hardening characteristics of materials under cyclic loading at elevated temperatures.

Preliminary inelastic strain comparisons between isothermal and thermomechanical experimental data have proven useful in developing a better understanding of thermomechanical material response for Hastelloy-X. From these types of comparisons it appears that general thermomechanical material behavior can be extracted from isothermal experimental data, but information concerning changes in material strain hardening behavior must come from thermomechanical test data. Further work is continuing to formulate a scheme to calculate the inelastic strain rate response.

FUTURE WORK

The emphasis of future work will be directed at simplifying the constant tables. For example, this can be accomplished by formulating relationships that are functions of cycle numbers. Once this idea has been investigated and worked out, the rest of the isothermal data base that has been collected for Hastelloy-X at NASA Lewis Research Center will be condensed into tabular form, and published in a report.

Future emphasis for thermomechanical deformation tests will entail completing a data base for thermal cycles involving a 200 °C temperature range and repeating some of the earlier experiments. As was stated in previous sections, the fitting routine for inelastic strains of thermomechanical tests will be formulated. It is anticipated that careful analysis of this data will provide insight towards differences in strain hardening behavior that exists between isothermal and thermomechanical loading.

REFERENCES

1. Sheffler, K.D. and Doble, G.S.: Influence of Creep Damage on the Low Cycle Thermal-Mechanical Fatigue Behavior of Two Tantalum Base Alloys. (TRW ER-7592, TRW, Inc.; NASA Contract NAS3-13228) NASA CR-121001, 1972.

2. Halford, G.R. and Manson, S.S.: Life Prediction of Thermal-Mechanical Fatigue Using Strainrange Partitioning. Thermal Fatigue of Materials and Components, ASTM STP-612, D.A. Spera and D.F. Mowbray, eds., ASTM, 1976, pp. 239-254. (NASA TM X-71829.)

3. Kuwabara, K.; Nitta, A.; and Kitamura, T.: Thermal–Mechanical Fatigue Life Prediction in High–Temperature Component Materials for Power-Plant. Advances in Life Prediction Methods, D.A. Woodford and J.R. Whitehead, eds., ASME, 1983, pp. 131–141.

4. Bartolotta, P.A.: Thermomechanical Cyclic Hardening Behavior of Hastelloy-X. NASA CR–174999 (University of Akron), November 1985.

5. Ellis, J.R.; Bartolotta, P.A.; Allen, G.P.; and Robinson, D.N.: Turbine Engine Hot Section Technology 1986, NASA CP–2444, October 1986, p. 293.

6. Bartolotta, P.A. and McGaw, M.A.: A High Temperature Fatigue and Structures Testing Facility. NASA TM–100151, August 1987.

TABLE I

TABLE OF CURVE-FITTING CONSTANTS FOR THE UPPER HALF OF THE HYSTERESIS LOOP OF A 425 °C ISOTHERMAL TEST; E = 175.149 GPa

CYCLE	C1	B1	A1	D2	C2	B2	A2	TIME, sec
5	0.651	-12.113	-1496.782	-0.003560	1.357	-24.342	-1441.291	9.310
10	.576	-10.729	-1449.155	-.002911	1.268	-22.875	-1393.738	9.319
20	.579	-12.123	-1382.321	-.003571	1.324	-26.542	-1308.885	10.470
100	.435	-10.250	-1253.793	-.002087	1.154	-26.345	-1160.644	11.787
200	.470	-10.804	-1188.877	.000275	.898	-20.762	-1131.388	11.504
500	.373	-10.178	-1079.978	.000230	.900	-24.708	-980.446	13.659
1000	.303	-8.846	-974.562	.002743	.628	-20.052	-888.642	14.576
2000	.305	-9.442	-827.634	.007796	.075	-7.920	-824.936	15.487
5000	.229	-11.505	-579.182	.006213	.278	-25.693	-351.876	25.109

CD-87-29304

TABLE II

TABLE OF CURVE-FITTING CONSTANTS FOR THE LOWER HALF OF THE HYSTERESIS LOOP OF A 425 °C ISOTHERMAL TEST; E = 175.149 GPa

CYCLE	C1	B1	A1	D2	C2	B2	A2	TIME, sec
5	-0.583	7.940	1206.806	0.000548	-1.015	13.748	1187.124	6.808
10	-.625	9.901	1145.612	.001955	-1.132	17.552	1115.806	7.918
20	-.504	8.509	1093.498	.000678	-1.004	16.801	1058.730	8.435
100	-.512	10.756	957.700	.000437	-.967	20.176	908.463	10.508
200	-.453	10.288	900.838	-.000190	-.895	20.381	843.457	11.343
500	-.305	8.310	818.786	.000165	-.928	25.195	704.034	13.616
1000	-.276	8.474	735.091	-.001950	-.721	23.515	616.127	15.350
2000	-.243	7.972	623.451	-.006956	-.169	11.144	582.133	16.391
5000	-.206	9.400	443.576	-.011082	.345	1.541	467.496	22.798

CD-87-29305

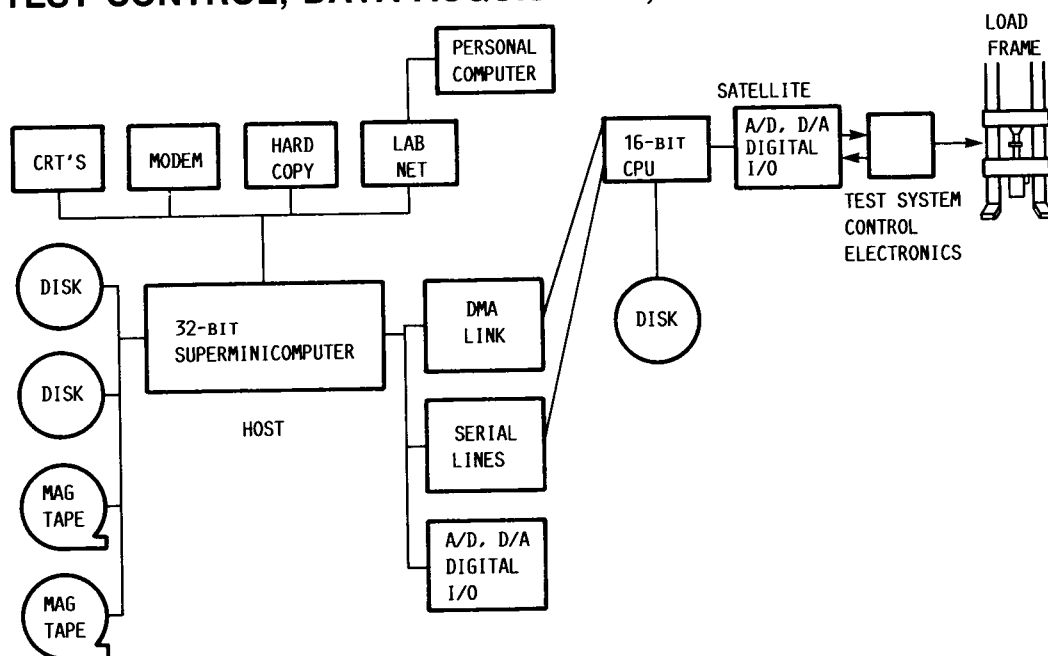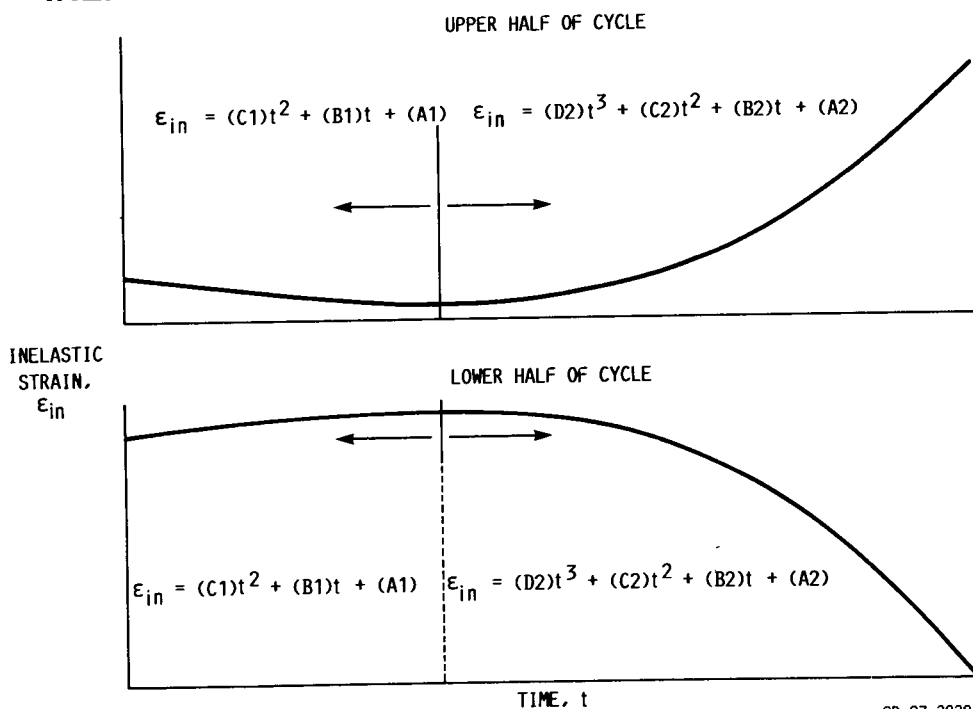# SCHEMATIC OF COMPUTER TEST SYSTEM SHOWING KEY ELEMENTS FOR TEST CONTROL, DATA ACQUISITION, AND DATA MANIPULATION

Figure 1

CURVE-FITTING APPROACH ILLUSTRATED BY TYPICAL INELASTIC STRAIN-TIME RESPONSES OF A CYCLE

UPPER HALF OF CYCLE

$\varepsilon_{in} = (C1)t^2 + (B1)t + (A1)$ $\varepsilon_{in} = (D2)t^3 + (C2)t^2 + (B2)t + (A2)$

INELASTIC STRAIN, ε_{in}

LOWER HALF OF CYCLE

$\varepsilon_{in} = (C1)t^2 + (B1)t + (A1)$ $\varepsilon_{in} = (D2)t^3 + (C2)t^2 + (B2)t + (A2)$

TIME, t

CD-87-29294

Figure 2

310

COMPARISON OF EXPERIMENTAL AND FITTED DATA DETERMINED UNDER ISOTHERMAL CYCLIC LOADING FOR CYCLE 10 (425 °C)

MATERIAL, HASTELLOY-X
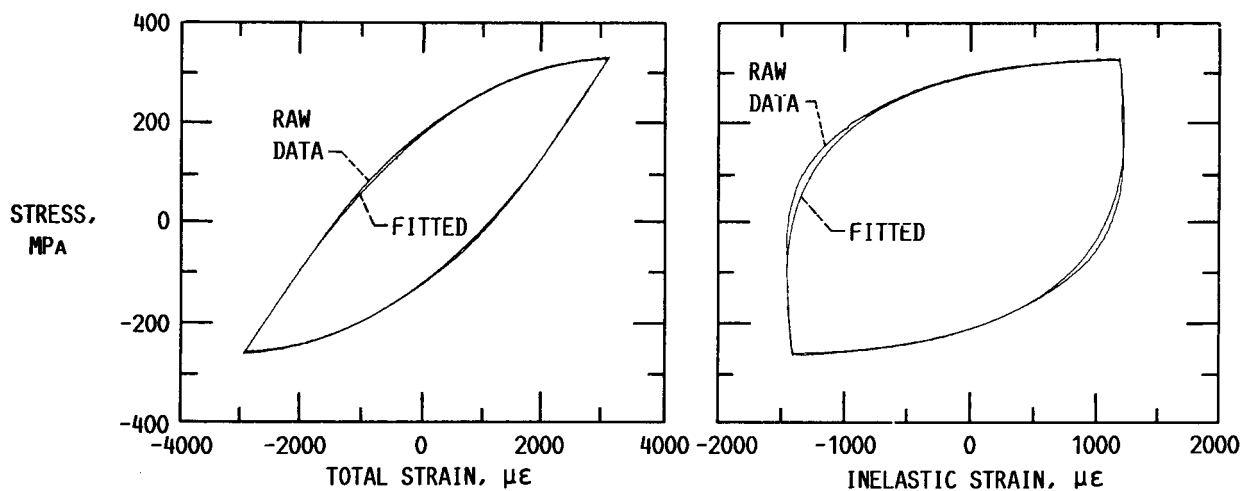
Figure 3

CD-87-29295

COMPARISON OF EXPERIMENTAL AND FITTED DATA DETERMINED UNDER ISOTHERMAL CYCLIC LOADING FOR CYCLE 100 (425 °C)
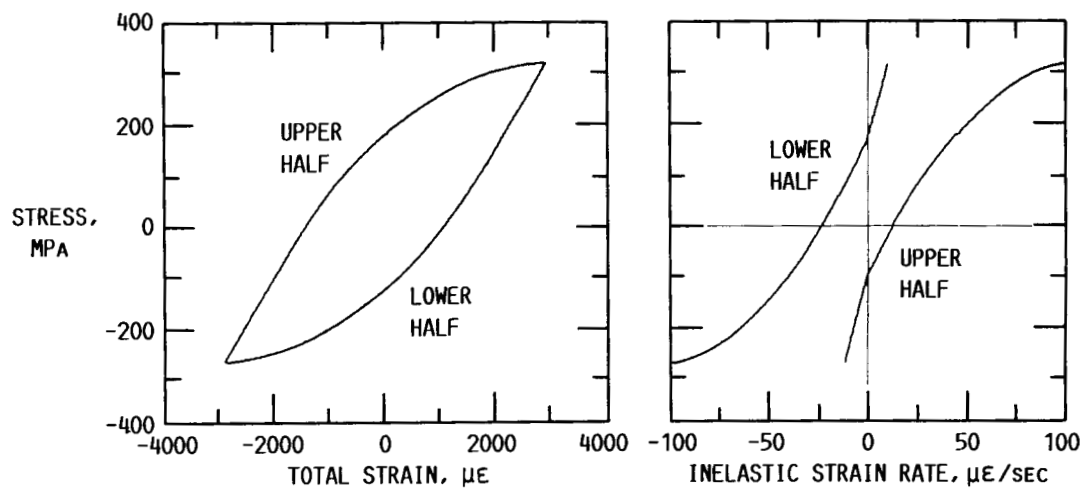
MATERIAL, HASTELLOY-X
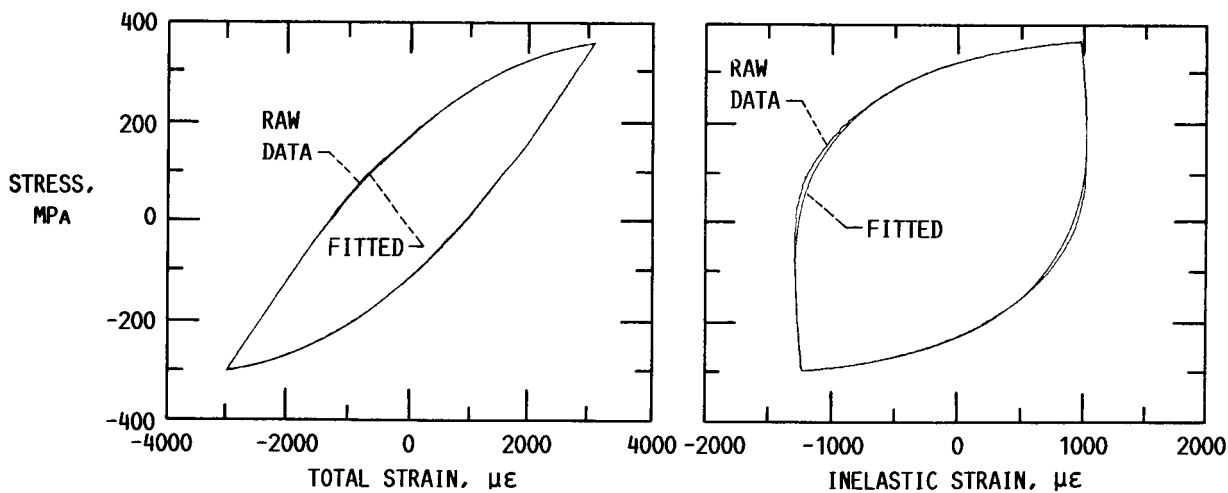
Figure 4

CD-87-29296

COMPARISON OF EXPERIMENTAL AND FITTED DATA DETERMINED UNDER ISOTHERMAL CYCLIC LOADING FOR CYCLE 5000 (425 °C)

MATERIAL, HASTELLOY-X
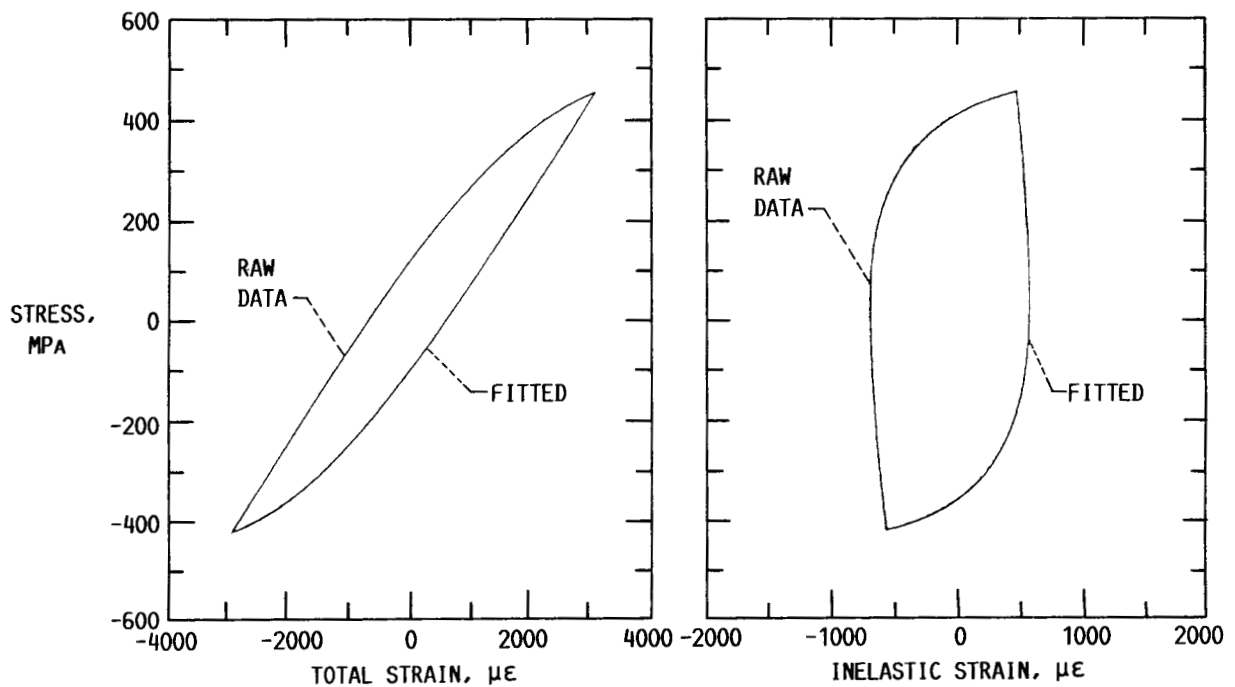
Figure 5

CD-87-29297

INELASTIC STRAIN RATES DEVELOPED DURING CYCLIC LOADING FOR CYCLE 10 (425 °C)

MATERIAL, HASTELLOY-X

CD-87-29298

Figure 6

INELASTIC STRAIN RATES DEVELOPED DURING CYCLE LOADING FOR CYCLE 100 (425 °C)
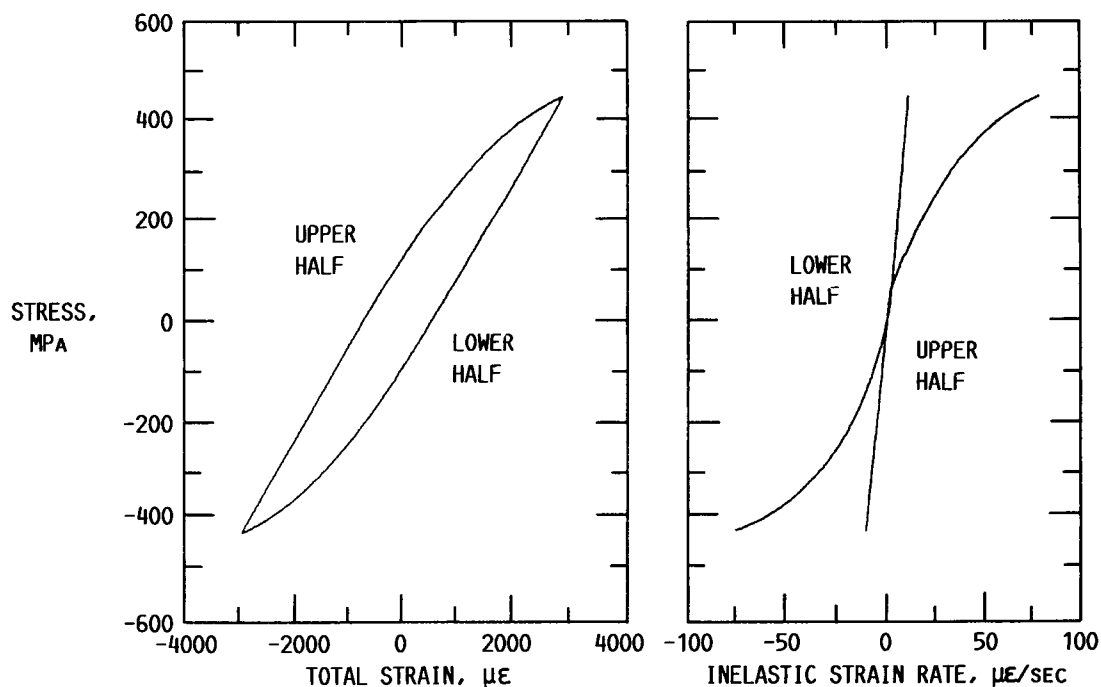
MATERIAL, HASTELLOY-X
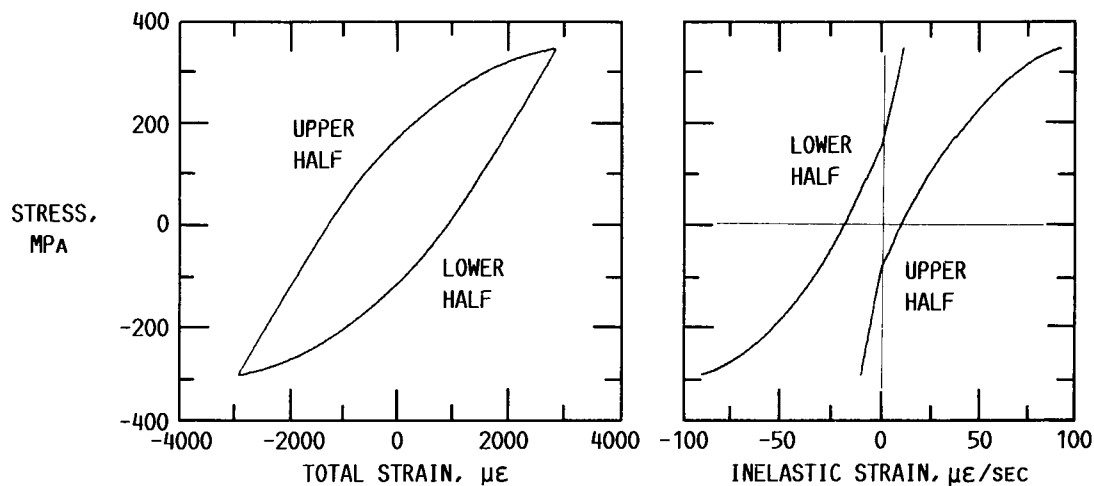
Figure 7

CD-87-29299

INELASTIC STRAIN RATES DEVELOPED DURING CYCLIC LOADING FOR CYCLE 5000 (425 °C)

MATERIAL, HASTELLOY-X

CD-87-29300

Figure 8

313

COMPARISON OF MATERIAL RESPONSE DETERMINED UNDER ISOTHERMAL AND THERMOMECHANICAL CYCLIC LOADING FOR CYCLE 10
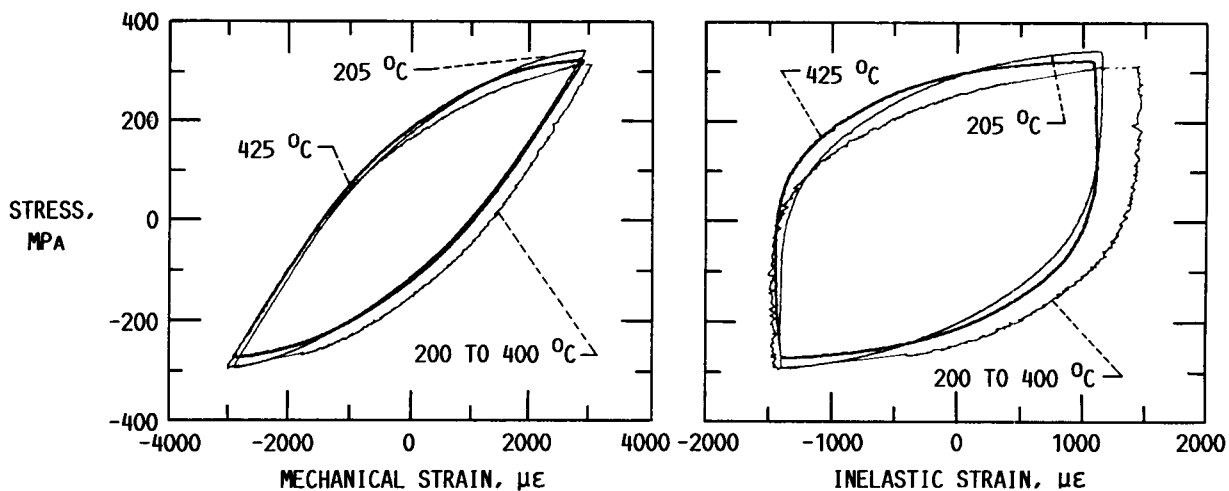
MATERIAL, HASTELLOY-X

Figure 9

CD-87-29301

COMPARISON OF MATERIAL RESPONSE DETERMINED UNDER ISOTHERMAL AND THERMOMECHANICAL CYCLIC LOADING FOR CYCLE 100
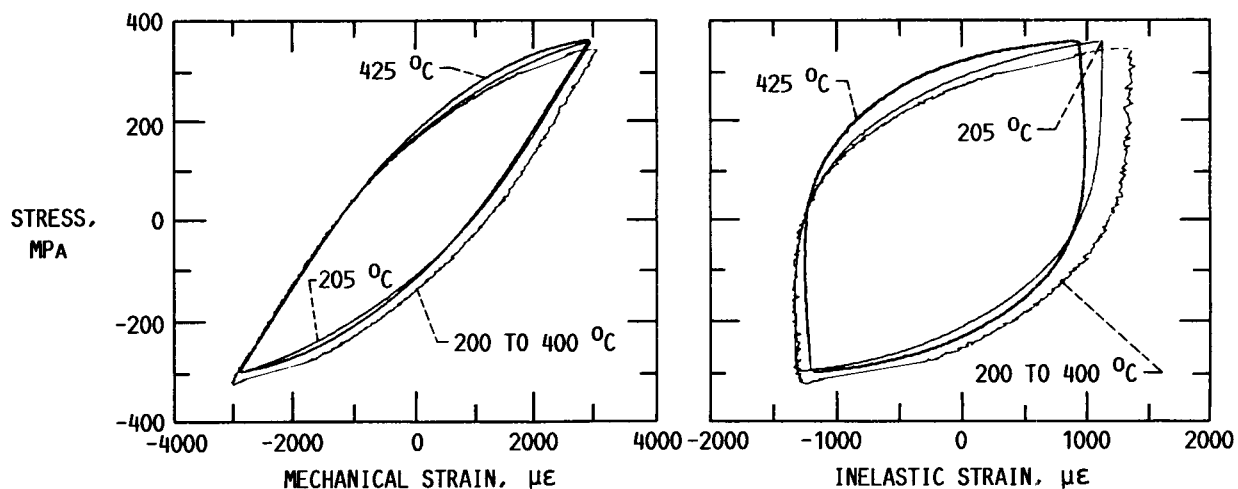
MATERIAL, HASTELLOY-X

CD-87-29302

Figure 10

314

COMPARISON OF MATERIAL RESPONSE DETERMINED UNDER ISOTHERMAL AND THERMOMECHANICAL CYCLIC LOADING FOR CYCLE 5000

MATERIAL, HASTELLOY-X

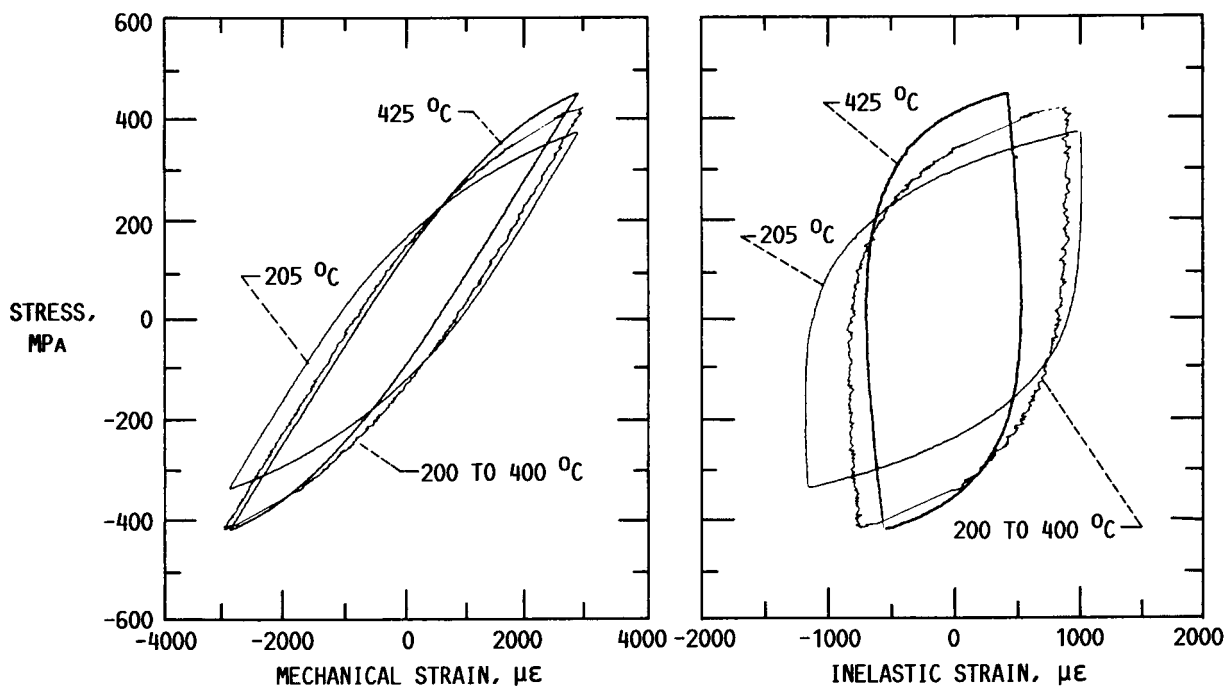Figure 11

CD-87-29303